Electrical conductivity and relaxation in poly(3-hexylthiophene)

Jan Obrzut[*] and Kirt A. Page

Polymers Division, National Institute of Standards and Technology, Gaithersburg, Maryland 20899, USA
(Received 31 May 2009; revised manuscript received 18 August 2009; published 25 November 2009)

We studied the complex conductivity of regioregular poly(3-hexylthiophene) (P3HT) in the temperature range between 193–333 K (−80 °C to 60 °C) and in the frequency range from the direct current (dc) to 12 GHz. The identified relaxation process was investigated by quasielastic neutron scattering (QENS). The dielectric loss peak extracted from complex conductivity corresponds to local molecular motions having an activation energy of about 9 kJ/mol, which agrees well with the QENS results. The molecular motions of the hexyl side groups in poly(3-hexylthiophene) contribute to this relaxation process in P3HT, which is coupled with a cooperative charge transport along the P3HT chains. In the cutoff frequency range, the real part of complex conductivity (σ') gradually transitions to a frequency-independent conductivity (σ'_∞), which is thermally activated. The activation energy of σ' at 50 MHz is about 80 meV. In comparison, the activation energy of the dc conductivity, σ_0, is larger, about 280 meV, while the value of σ_0, is many orders of magnitude smaller than σ'_∞. We conclude that the local relaxation of the hexyl side groups contribute to a topological disorder in the polymer structure. As a consequence the energy barriers of the charge transport increase and the conductivity decreases. At 190 K the conductivity decreases from the disorder-free σ'_∞ of approximately 5×10^{-4} S/m to σ_0 of about 1×10^{-9} S/m.

I. INTRODUCTION

Organic semiconductors have generated great interest due to their potential use in thin-film transistors, light-emitting diodes, photoelectrical cells, and other electronic applications.[1–3] Development of these materials has revealed some unique electrical and processing characteristics. Functionalized polythiophenes exemplify the feasibility of achieving desired properties by tailoring chemical structures. For example, ambipolar transport was achieved in a thin-film transistor using a quinoid oligothiophene derivative.[4] Likewise, a hybrid semiconductor composed of thiophene and acene molecules showed improved environmental stability and increased mobility.[5] Oligothiophenes and polythiophenes, including poly(3-hexylthiophene) (P3HT), show some of the highest carrier mobilities among organic electronic materials.[6,7] Studies of P3HT reveal a tendency to self-organization by forming a semicrystalline domain embedded in an amorphous matrix.[8] In comparison to polyacenes, the backbone structure of polythiophenes is less rigid, with the additional flexibility arising from the torsional motion of its thiophene rings.[9] As a result, polythiophene shows larger deviation from planarity and lower hole mobility along chains than poly(phenylene vinylene).[10,11] In P3HT, besides interring torsional motion, the mobility of the hexyl pendant group introduces additional complexity to the charge transport that becomes coupled with conformational dynamics and dielectric relaxation. Relaxation of electronic states coupled to low-energy interring torsional motions results in low-frequency relaxation[11,12] which apparently occurs cooperatively. This, unfortunately, makes it difficult to separate the relaxation process of molecular reorientation from polarization of the relatively low-mobility charge carriers.

The frequency dependence of conductance has significant implications on the performance of devices such as field-effect transistors (FET) (Ref. 13) and metal-insulator-semiconductor (MIS) memory cells,[14,15] all of which require alternating current (ac) operation. In the case of MIS capacitors, with a P3HT film as the active semiconductor, Taylor *et al.*[15] extracted the complex admittance of P3HT from an equivalent circuit model of the device in the accumulation and depletion states. In the case of FET, Lenski *et al.*[13] used a resistance capacitance (RC) transmission line model to extract the frequency-dependent complex conductance of the pentacene film as an active semiconductor. These two approaches give model-dependent solutions, which require a number of adjustable parameters and simplifying assumptions.[13,15]

In this paper, we choose P3HT as a representative organic semiconducting material, for which we quantify the intrinsic direct current (dc) and ac conductivity and the dielectric relaxation response, directly. We analyze the relaxation behavior of the side chains in P3HT by employing quasielastic neutron scattering (QENS).[16,17] The QENS technique takes advantage of the relatively large incoherent-scattering cross section of hydrogen atoms, which are located predominantly on the pendant hexyl group. Our measurements and analysis technique seeks to improve the fundamental understanding of the dielectric and conductivity properties of organic semiconducting materials in the broad frequency range.

II. MATERIALS AND MEASUREMENTS

High-purity (99.995%) poly(3-hexylthiophene) with a molecular weight of about 40 kD and head-to-tail regioregularity >99% was obtained from Plextronics in form of flakes and was used during analysis without further purification. Differential scanning calorimetry (DSC) thermograms taken under nitrogen during heating at a rate of 10 K/min showed a melting temperature of about 242 °C with recrystallization upon cooling at about 193 °C. These results are consistent with the semicrystalline structure of P3HT.[18–20] In the tem-

TABLE I. dc conductivity (σ_0) of P3HT as a function of temperature (T).

T (K)	σ_0 (S/m)
191.8	1.403×10^{-9}
202.8	3.661×10^{-9}
214.2	8.151×10^{-9}
222.9	1.971×10^{-8}
233.3	3.887×10^{-8}
241.9	7.521×10^{-8}
254.1	1.370×10^{-7}
263.4	2.170×10^{-7}
272.4	3.149×10^{-7}
282.6	4.690×10^{-7}
293.2	6.780×10^{-7}
303.1	9.486×10^{-7}
313.0	1.184×10^{-6}
322.1	1.470×10^{-6}
331.5	1.830×10^{-6}

perature range between −80 °C and 70 °C, where our electrical measurements take place, the DSC thermo grams do not reveal any apparent glass transition. In the case of regioregular P3HT the amount of the amorphous phase is considered very small and the heat capacity from a glass transition is hardly visible in DCS.[19] We note that thermal annealing and processing from solution considerably affect the morphology of P3HT. Depending on the thermal history, regioregularity, synthetic route, molecular weight and processing conditions, P3HT films may show glassylike transitions from nonequilibrium structures in a broad range of temperatures.[21,22]

For the electrical measurements, ohmic contacts were made with gold electrodes. The gold electrodes, with a diameter of 3.0 mm and a thickness of 0.1 μm, were evaporated in vacuum on both sides of the P3HT films. The thickness of the films was between 40 μm and 50 μm, measured with an uncertainty of ±1 μm. To avoid oxygen doping and moisture contamination all samples were handled either under a nitrogen or argon inert-gas atmosphere in a dry box. The measurements were carried out at isothermal conditions in a temperature range of 333–193 K (+60 °C to −80 °C). Each constant temperature was reached during cooling from 70 °C at a rate of 0.5 °C/min. During the measurements, the specimen temperature was controlled to within ±0.5 K. The direct constant current (dc) conductivity σ_0 was determined from the linear and symmetric current-voltage (I-V) characteristics measured by sourcing a small current using a Keithley-6360 source meter. The constant current was increased in steps, each having duration of about 2 s. The conductivity σ_0 was determined from the slope of the I-V plots, $I = \sigma_0 \frac{A}{d} V$, where d is the sample thickness and A represents the area of the top electrode. The voltage drop maximum was kept within ±1 V. The temperature-dependent σ_0 results are shown in Table I. In the frequency range of 40 Hz to 100 MHz, measurements of complex impedance, Z^*, (im-

pedance magnitude $|Z^*|$ and phase angle φ) were carried out using an Agilent 4294A Precision Impedance Analyzer at the oscillator amplitude of ±500 mV. At higher frequencies, in the range of 100 MHz to 12 GHz, the complex impedance Z^* was obtained from one-port measurements of the scattering parameter, S_{11} using a HP 8720D vector network analyzer,[23,24] $Z^* = Z_0(1 + S_{11})/(1 - S_{11})$, where $Z_0 = 50$ Ω is the characteristic impedance of the standard transmission line. The combined relative experimental uncertainty of the measured complex impedance magnitude was within 4% while the experimental resolution of the phase-angle measurements was within 0.5°.

The complex conductivity, $\sigma^* = \sigma' + j\sigma''$, was obtained from the measured complex impedance, Z^*, normalized by the geometry of the test specimen,

$$\sigma^* = \frac{d}{Z^* A}, \tag{1}$$

where d is again the sample thickness and A represents the area of the top electrode. The complex conductivity of molecular solids, such as organic semiconductors, can be analyzed in terms of the lumped element model, in which the conducting and dielectric properties are represented by a network of idealized resistors, R, and capacitors with complex capacitance, C^* The equivalent complex admittance, Y^*, is the sum of the admittances of these two elements, shown below[25–27]

$$Y^* = 1/R + j\omega C^*. \tag{2}$$

Accordingly, the complex conductivity, σ^*, of a specimen with a thickness (d) and an active area of electrodes can be expressed by Eq. (3).

$$\sigma^* = \sigma_0 + j\omega\varepsilon_0\varepsilon_r^*, \tag{3a}$$

where σ_0 is frequency independent dc conductivity, $\omega = 2\pi f$ is the angular frequency, and ε_r^* is the complex relative dielectric permittivity of the material where $\varepsilon_r^* = \varepsilon_r' - j\varepsilon_r''$. ε_0 is the dielectric permittivity of free space and $j^2 = -1$. Separating Eq. (3a) into real and imaginary components we obtain

$$\sigma' = \sigma_0 + \omega\varepsilon_0\varepsilon_r'' \tag{3b}$$

and

$$\sigma'' = j\omega\varepsilon_0\varepsilon_r'. \tag{3c}$$

Thus, the scaling of the in-phase component of the complex conductivity (σ') with frequency is contingent on the frequency dependence of the imaginary part of the dielectric constant, $\varepsilon_r''(\omega)$. The frequency dependence of the real part of the dielectric permittivity $\varepsilon_r'(\omega)$ determines the scaling of σ''. We note that the complex (ac) conductivity has also been described in terms of the complex modulus notation[28] and was used to interpret the ac conductivity of poly(3-alkylthiophene)s.[29] However this interpretation invokes a correlation of unrelaxed dielectric permittivity (ε_∞) with σ_0, which is unrelated to σ' [see Eq. 4 in Ref. 29]. In our present approach the complex admittance is a sum of the pure imaginary (dielectric) contribution and the real contribution from σ_0 and σ', respectively. Thus ε_∞ and σ_0, which

describe different physical effects, are interpreted separately.

QENS measurements were carried out using the NG2 high-flux backscattering spectrometer at the NIST Center for Neutron Research (NCNR) in Gaithersburg, MD. The elastic scattering was measured with the instrument in fixed-window mode over a temperature range from 50 to 550 K at a heating rate of 1 K/min. For dynamic measurements, the instrument was operated in the dynamic range of $\pm 17 \ \mu$eV.[30] The dynamic scans were used to determine the instrument resolution, Γ_r, which is a crucial component in the fitting of the experimental data. The temperature dependence of the elastic-scattering intensity, $S(Q)$, was analyzed using the following equation[31,32]

$$S(Q, \omega \approx 0) = \exp\left(\frac{-\langle r^2 \rangle Q^2}{3}\right)\left\{ A_o(Q) + \frac{2}{\pi}[1 - A_o(Q)]\arctan\left(\frac{\Gamma_r}{\Gamma}\right)\right\}. \quad (4)$$

In Eq. (4), Q is the scattering wave vector, $Q = (4\pi/\lambda)\sin\theta$, λ is the wavelength of the neutron beam, 2θ is the scattering angle, $A_o(Q)$ is the elastic incoherent structure factor, Γ_r is the width of the resolution function, and Γ is the width of a Lorentzian distribution that describes the quasielastic broadening. The exponential term in Eq. (4) represents the Debye-Waller factor (DWF), which describes the decrease in the elastic-scattering intensity with increasing temperature. The origins of this decrease in elastic intensity can be attributed to molecular vibrations when no other molecular motions (i.e., rotational or translational) are present. In the DWF, $\langle r^2 \rangle$ is the mean-square displacement of the scattering centers. At temperatures below 100 K, the width of the quasielastic component is less than that of Γ_r. With increasing temperature above 100 K, the width of the quasielastic component broadens. From the fit of Eq. (4) to the fixed-window data, we determined Γ, which follows the Arrhenius law: $\Gamma = \Gamma_0 \exp(-E_a/RT)$, where Γ_0 is a temperature-independent prefactor (adsorbing an attempt frequency factor and an entropy activation term) and E_a is the activation energy for the process giving rise to the quasielastic scattering.

III. RESULTS

A. Electrical conductivity

Figure 1(a) shows the real part (σ') of the complex conductivity as a function of frequency plotted at several temperatures from 193 to 333 K ($-80\ °$C to 60 $°$C) in increasing steps of 10 K. At the lowest frequencies and moderate temperatures, the general trend is that σ' coincides with σ_0. At room temperature the dc conductivity σ_0 is about 6.77 $\times 10^{-7}$ S/m (Table I). Figure 1(b) indicates that σ_0 increases exponentially with temperature with activation energy of about 0.26 eV, where the pre-exponential factor is about 2.1×10^{-2} S/m. Within the investigated temperature range, the plot of $\ln(\sigma_0)$ vs $1/T$ is fairly linear up to 300 K. In particular, there is no evidence of a decrease in the activation energy of σ_0 at lower temperatures, which be indicative of a transition from a hopping transport to conduction in semime-
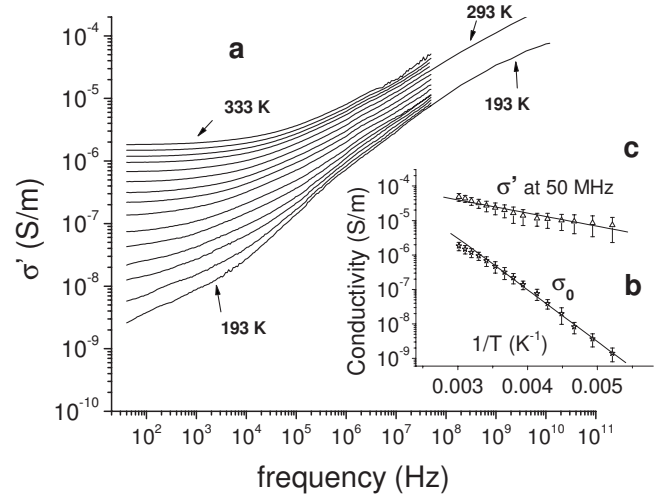

FIG. 1. (a) Conductivity (σ') as a function of frequency plotted at several temperatures from 193 to 333 K in increasing steps of 10 K. (b) Conductivity σ_0 as a function of $1/T$. Line represents a fit to the Arrhenius expression where the activation energy is about 0.28 eV. (c) Conductivity σ' at 50 MHz as a function of $1/T$. The line represents a fit to the Arrhenius expression where the average activation energy is about 80 meV.

tallic extended states.[33] Such transition was reported for P3HT under electrostatic charge injection at low temperatures[7] where the activation energy for dc conduction approached the metallic range of about 4 meV. Our σ_0 data are more in accordance with earlier results reported by van de Leur *et al.*[34,35] for neutral P3HT. At higher temperatures the plot in Fig. 1(b) changes slope above 300 K showing somewhat depressed σ_0 values. Such a trend seems to be consistent with the thermally liberated local structural changes in the polymer matrix, indicating a "*twits glass transition*" of thiophene rings, at about 300 K in P3HT using FT-IR and NMR spectroscopy.[19,36]

It is seen in Fig. 1(a) that σ' exhibits a plateau at low frequencies that persists from dc up to the relaxation frequency ω_s. In the multiple hopping regime between ω_s and the microscopic cutoff frequency ω_∞ ($\omega_s < \omega < \omega_\infty$), conduction occurs at sites in isolated clusters, and σ' increases with ω, apparently in accordance with approximate power-law behavior $[\sigma'(\omega) - \sigma_0 \sim \omega^n]$.[37–39] The relaxation frequency, $\omega_s = \rho\sigma_0/\Delta\varepsilon$, depends on the distribution of the hopping conductivity sites in disordered materials, i.e., it reflects the resistance between hopping sites and effective capacitance. It thus scales accordingly with σ_0 and the dielectric loss strength $\Delta\varepsilon$.[37,40] The exponent n obtained from the linear portion of the σ' plots above ω_s, increases with decreasing temperature from about 0.42 at 333 K to 0.7 at 193 K, indicating that the long-range order in electronic states increases considerably with decreasing temperature. Assuming that this trend continues at temperatures below 193 K, n would approach the value of an amorphous silicon[41,42] $n \approx 0.8$ at about 180 K. We note that in the vicinity of ω_s the exponent n increases with frequency rather than decreases, suggesting that the transport mechanism in that frequency range can be better explained in terms of the effective-medium approximation model[43,44] rather than by the hopping-pair approxi-
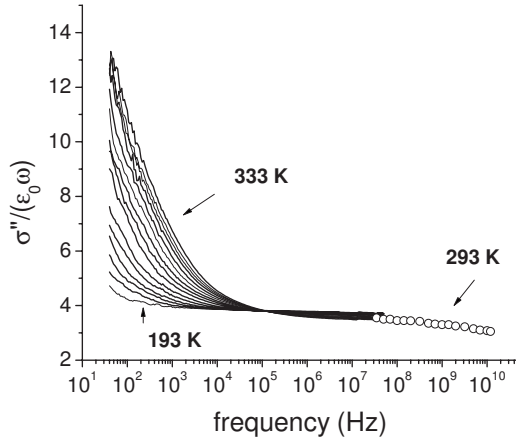
FIG. 2. Conductivity $[\sigma''/(\varepsilon_0\omega)]$ plotted in dielectric notation. The plots represent the real part of the dielectric permittivity (ε_r') as a function of frequency at several temperatures from 193 to 333 K in increasing steps of 10 K.

mation model.[33] Figure 1(a) shows that with increasing frequency σ' becomes significantly less temperature dependent than σ_0. At 50 MHz the average activation energy for σ' decreases to about only 80 meV [see Fig. 1(c)]. Perhaps our most interesting finding, however, is a gradual transition of σ' from the power law to a frequency-independent conductivity (σ_∞') that we observe around 50 MHz. Although our microwave measurements are less accurate at low temperatures due to the lack of suitable calibration standards, we can still qualitatively estimate $\sigma_\infty' \approx 5 \times 10^{-5}$ S/m and the cutoff frequency ω_∞ to be in the range of about 10^{11} Hz at 193 K.

In Fig. 2 we plot the imaginary part (σ'') of the complex conductivity using dielectric notation, $\sigma''/(\varepsilon_0\omega)$, which represents the dielectric constant, ε_r', [see Eq. (3b)]. Figure 2 shows that ε_r' decreases with increasing frequency. The inflection point seen at about 50 kHz can be attributed to the increasing density of P3HT on cooling. The apparent coefficient of thermal expansion determined from the dependence of ε_r' on temperature at 100 MHz is about 2.15×10^{-3}/deg. In the high-frequency limit of 12 GHz, the dielectric constant of P3HT at room temperature decreases to about 3.0, which is comparable to the value estimated from the refractive index of 3-hexylthiophene.[35] A rapid decrease in ε_r' seen between dc and 10 kHz is indicative of a dielectric relaxation process in that frequency range. Since the σ_0 and σ' were determined in separate measurements, we extracted the dielectric loss, ε_r'' directly from the real part of the complex conductivity [Eq. (3b)] data, $\varepsilon_r'' = \sigma' - \sigma_0/\omega\varepsilon_0$. Such an approach does not require any prior assumption about the character or number of the dielectric processes and it can unambiguously identify the dielectric relaxation in the presence of a large conductance. However, the method is limited in the low-frequency range, as when σ' approaches the value of σ_0 the uncertainty in ε_r'' becomes large. The ε_r'' is shown as a function of frequency at several temperatures in Fig. 3(a). Although the complex dielectric permittivity that we obtained can be fitted to a relaxation function such as Havriliak and Negami[45] for the relaxation time, here, we simply assumed that $\tau \approx 1/f_{max}$, where f_{max} was obtained from the peak value of ε_r'' shown in Fig. 3(a).
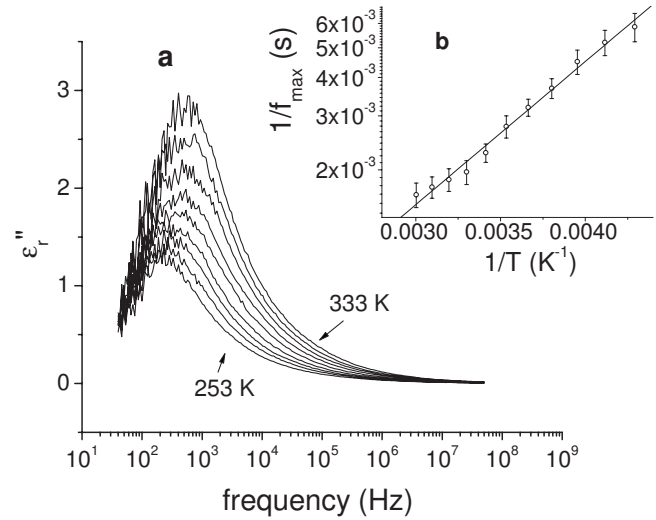

FIG. 3. (a) Dielectric loss ε_r'' as function of frequency at several temperatures from 253 to 333 K in steps of 10 K. (b) Plot of $1/f_{max}$ as a function of temperature. Line represents a fit to the Arrhenius expression.

The temperature dependence of the dielectric relaxation time, τ, is shown in Fig. 3(b). The symbols correspond to τ data while the line represents a linear regression through the experimental points. The dielectric relaxation process obeys the Arrhenius relation well with an activation energy, E_a, of about 9 kJ/mol and a pre-exponential factor 5.9×10^{-5}. The value of E_a for P3HT is significantly lower than an activation energy that would typically correspond to secondary β relaxation in polar organic polymers, (20–50 kJ/mol).[46] This indicates that the relaxation process in P3HT has a very local character[47] comparable to that of the hexyl group. Since the hexyl groups in P3HT are not polar and are dielectrically inactive, we performed quasielastic neutron-scattering measurements to investigate the energy scale of this molecular process and whether it is coupled to the charge-carrier relaxation of P3HT.

B. Quasielastic neutron scattering

Previous studies have shown that QENS is useful in studying both molecular motions in polymers associated with the secondary local β relaxation, as well as with the cooperative α relaxation.[32,48,49] The QENS technique is specifically sensitive to the motions of hydrogen atoms due to their large incoherent-scattering cross section. In P3HT, there are 13 hydrogen atoms on the side chain and only one hydrogen atom on the backbone per repeating unit. It is therefore possible to use QENS to selectively monitor the contribution of the side chains to the molecular dynamics in this material. The normalized elastic-scattering intensity as a function of temperature is shown in Fig. 4(a) at a scattering wave-vector value of $Q = 0.99$ Å^{-1} ($Q = 2\pi/d$, where d is the length scale of the motion). The solid line is a fit of the experimental scattering data to Eq. (4). This particular Q value corresponds to molecular motions with a length scale of approximately 0.6 nm, which is comparable to length scales associated with the hexyl side group.[20,48] The activation energy of
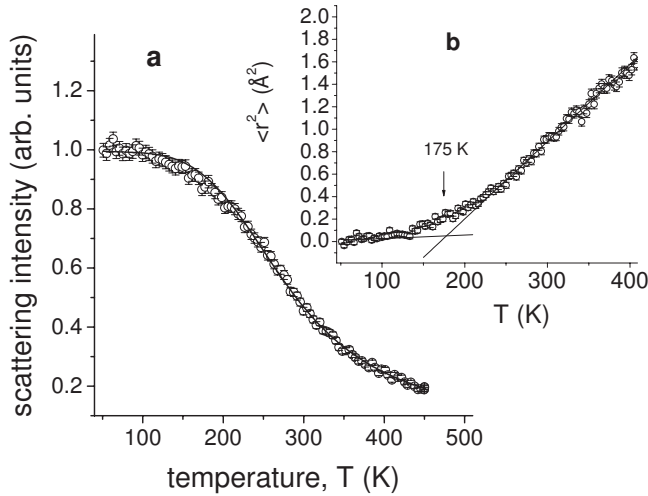
FIG. 4. (a) Normalized elastic-scattering intensity as a function of temperature at $Q \approx 0.99$ Å^{-1}. The solid line represents a fit of the data to Eq. (4) using an instrument resolution of 0.86 meV as determined from the dynamic scan at 50 K. (b) Mean-square displacement, $\langle r^2 \rangle$ for P3HT as measured by QENS.

the hexyl group motions as determined from Eq. (4), is about 8 ± 1 kJ/mol, which agrees very well with the value determined from the measurement of the dielectric relaxation time in P3HT. It is seen that the elastic intensity in Fig. 4(a) begins to change slope again at the temperature of about 300 K. This indicates a more cooperative process that may correspond to a (sub Tg) relaxation in P3HT, such as a twist glass transition.[19] In Fig. 4(b) we plotted the natural log of the elastic-scattering intensity as a function of Q^2 at each temperature, from which we determined the mean-square displacement of the hydrogen atoms. The change in the mean-square displacement with temperature, $d\langle r^2 \rangle / dT$, is $2.97 \pm 0.5 \times 10^{-4}$ Å^2 K^{-1}, agrees with values reported for other polymeric systems.[49] The motions of hexyl groups are liberated at about 175 K, which is reflected in Fig. 4(b) as a change in the slope of the $\langle r^2 \rangle$ plot at that temperature. The plateau seen in Fig. 4(b) at the lowest temperatures indicates that the molecular motions become negligibly small below 175 K. This is consistent with our earlier finding that the long-range order in electronic states increases considerably with decreasing temperature and would approach that of amorphous silicon below 180 K.

IV. DISCUSSION

Partially ordered (e.g., semicrystalline) organic semiconductors such as P3HT form an important class of soft materials. Disorder contributes to the localization of electronic states and influences the charge transport within these materials.[50] The characteristic time of their molecular motion is comparable to that of their charge-carrier dynamics. It is, therefore, difficult to describe the charge transport of these material using either static disorder models or temperature-averaged electronic models. Recently, a model Hamiltonian using a combination of molecular-dynamics and quantum-chemical methods along with semiclassical correlations has

been proposed for such systems with considerable success.[51] We propose a different approach that allows us to directly separate the relaxation processes in the presence of large conductivity. The dielectric loss peak that we identified corresponds to very local molecular motions having an activation energy of about 9 kJ/mol, which agrees well with the QENS results. Both the dielectric and QENS results indicate that the molecular motions of hexyl side groups in poly(3-hexylthiophene) contribute to this relaxation process. The relatively long relaxation time, on the order of 10^{-3} s, suggests that the molecular relaxation process in P3HT cooperates considerably with low-mobility charge carriers. The relaxation of electronic states coupled with the molecular motions of thiophene rings results in a low-frequency relaxation having an activation energy of about 100 meV.[11,12]

Our results indicate that the relaxation effect of the side hexyl group on the charge polarization along the chains is also significant, and results in an increased level of disorder, which is manifested as a dispersion in conductivity. At 193 K, the conductivity decreases with decreasing frequency from the high-frequency plateau $\sigma'_\alpha \approx 10^{-5}$ S/m. to $\sigma_0 \approx 10^{-9}$ S/m. A similar form of disorder was found in amorphous semiconductors such as silicon and germanium,[52,53] where the dielectric loss arises from the inertia of the charge carriers having limited free path. In comparison, σ' in "disorder-free" single-crystal semiconductors have a flat frequency characteristic, $\sigma_0 \approx \sigma'_\alpha$, and no dielectric relaxation effects are seen up to microwave frequencies. The existence of the dielectric loss peak in neutral P3HT therefore indicates that conductivity of both σ_0 and σ' is governed by a similar transport mechanism. The complex conductivity shows a thermally activated Arrhenius response, which points to a hopping transport with a distribution of energy barriers,[54,55] well described by the effective-medium approximation model.[44] Accordingly, the dc conductivity activation energy is the maximum activation energy involved in the conduction process, which takes place on an infinite percolation cluster. At intermediate frequencies above ω_s were σ' increases strongly with frequency ($\sigma' \sim \omega^n$), the transport is dominated by hopping in finite clusters. The values of n (0.5–0.7) agree well with those obtained from the time-of-flight measurement of dispersive transport in P3HT.[56] The increase in conductivity [Fig. 1(a)] continues as long as the frequency of the field is lower than the hopping frequency of the charge carriers. A characteristic feature of this transport is that in the double logarithmic scale, plot of σ' vs frequency changes from a convex to a concave shape, which we indeed observe in Fig. 1(a) at the lowest temperatures. In the higher cutoff frequency range, n gradually decreases toward zero, σ' approaches the value of σ'_α, and the activation energy decreases to a minimum. Thus, the conductivity difference, $\sigma_0 - \sigma'_\alpha$, is the effective measure of disorder.

In organic semiconductor applications, it is important to realize that the onset frequency (ω_s) at which σ' begins to increase, the fractional exponent n and the activation energies of σ_0 and σ'_α evidently give basic information that can be used for the adjustment of the structural properties and to identify the limits in the electronic performance that can possibly be achieved. Within the large volume of literature published on P3HT, the primary focus has been almost exclu-

sively on achieving a high level of dc conduction through chemical modification and doping, neglecting the dynamic aspect of the charge transport. A proper understanding of the frequency dependent conductivity is important to correctly describe the dc charge transport. Using the frequency-dependent conductivity as guide, the goal of future materials engineering research should be to minimize the dielectric loss effects and shift ω_s toward ω_∞. A desirable result of such a materials modification would manifest as a decrease in the activation energy of the dc conduction toward a goal of approaching the activation energy of σ'_∞ along with an improvement in charge-carrier mobility at lower gate fields.

From this perspective, understanding the recent reports of investigators having achieved a low activation energy and metalliclike conduction under charge injection conditions and high gate fields,[57] would be aided considerably by modeling[50] and the evaluation of frequency-dependent charge transport.[13] Future work on organic semiconducting materials should consider the significance of frequency-dependent conductivity in relation to the characteristic field-effect mobility in order to better understand this important phenomenon from a more fundamental perspective.

V. CONCLUSION

We quantified the frequency-dependent conductivity and the dielectric relaxation in P3HT. The identified dielectric loss peak corresponds to very local molecular motions having an activation energy of about 9 kJ/mol, which agrees well with the QENS results. Both the dielectric and QENS results indicate that this relaxation process in P3HT can be attributed to molecular motions of the hexyl side groups in poly(3-hexylthiophene).

The local relaxation of the hexyl side groups contributes to a topological disorder in the polymer structure. As a consequence the conductivity decreases from the defect-free σ'_∞ of approximately 5×10^{-4} S/m to σ_0 of about 1×10^{-9} S/m at 190 K while the corresponding energy barriers of the charge transport increase. In the higher, cutoff frequency range, the exponent n decreases toward zero, and σ' gradually transitions to a frequency-independent conductivity (σ'_∞), which is thermally activated with an activation energy of σ'_∞ about 80 meV. In comparison, the activation energy of the dc conductivity, σ_0, is larger, about 280 meV, which is the maximum activation energy involved in the conduction process.

The characteristic parameters of the frequency-dependent conductivity, the onset frequency (ω_s) at which σ' begins to increase, the fractional exponent n and the activation energies of σ_0 and σ'_∞ evidently give basic information that can be used for the adjustment of the structural properties and to identify the theoretical limits of the charge transport.

*Corresponding author; jan.obrzut@nist.gov

[1] Z. T. Zhu, J. T. Mason, R. Dieckmann, and G. G. Malliaras, Appl. Phys. Lett. **81**, 4643 (2002).

[2] B. Crone, A. Dodabalapur, A. Gelperin, L. Torsi, H. E. Katz, and A. J. Lovinger, Appl. Phys. Lett. **78**, 2229 (2001).

[3] H. Sirringhaus, T. Kawase, R. H. Friend, T. Shimoda, M. Imbasekaran, W. Wu, and E. P. Woo, Science **290**, 2123 (2000).

[4] R. J. Chesterfield, C. R. Newman, T. M. Pappenfus, P. C. Ewbank, M. H. Haukaas, K. R. Mann, L. L. Miller, and C. D. Frisbie, Adv. Mater. (Weinheim, Ger.) **15**, 1278 (2003).

[5] V. Coropceanu, O. Kwon, B. Wex, B. R. Kaafarani, N. E. Gruhn, J. C. Durivage, D. C. Neckers, and J. L. Bredas, Chem.-Eur. J. **12**, 2073 (2006).

[6] A. Facchetti, M. Mushrush, M. H. Yoon, G. R. Hutchison, M. A. Ratner, and T. J. Marks, J. Am. Chem. Soc. **126**, 13859 (2004).

[7] M. J. Panzer and D. Frisbie, Adv. Funct. Mater. **16**, 1051 (2006).

[8] S. Malik and A. K. Nandi, J. Polym. Sci., Part B: Polym. Phys. **40**, 2073 (2002).

[9] G. R. Hutchison, M. A. Ratner, and T. J. Marks, J. Am. Chem. Soc. **127**, 2339 (2005).

[10] F. C. Grozema, P. T. van Duijnen, Y. A. Berlin, M. A. Ratner, and L. D. A. Siebbeles, J. Phys. Chem. B **106**, 7791 (2002).

[11] D. A. da Silva Filho, V. Coropceanu, D. Fichou, N. E. Gruhn, T. G. Bill, J. Gierschner, J. Cornil, and J. L. Bredas, Philos. Trans. R. Soc. London, Ser. A **365**, 1435 (2007).

[12] J. Du, Z. Wang, W. Feng, K. Yoshino, and T. Kobayashi, Phys. Rev. B **77**, 195205 (2008).

[13] D. R. Lenski, A. Southard, and M. S. Fuhrer, Appl. Phys. Lett. **94**, 232103 (2009).

[14] M. Lada, Appl. Phys. Lett. **93**, 143308 (2008).

[15] D. M. Taylor and N. Alves, J. Appl. Phys. **103**, 054509 (2008).

[16] D. Richter, Physica B **276-278**, 22 (2000).

[17] D. Richter, M. Monkenbusch, A. Arbe, and J. Colmenero, J. Non-Cryst. Solids **287**, 286 (2001).

[18] S. Pal and A. K. Nandi, J. Appl. Polym. Sci. **101**, 3811 (2006).

[19] K. Yazawa, Y. Inoue, T. Yamamoto, and N. Asakawa, J. Phys. Chem. B **112**, 11580 (2008).

[20] M. Brinkmann and P. Rannou, Macromolecules **42**, 1125 (2009).

[21] S. Hugger, R. Thomann, T. Heinzel, and T. Thurn-Albrecht, Colloid Polym. Sci. **282**, 932 (2004).

[22] J. Zhao, A. Swinnen, G. van Assche, J. Manca, D. Venderzande, and B. van Mele, J. Phys. Chem. B **113**, 1587 (2009).

[23] J. Obrzut and A. Anopchenko, IEEE Trans. Instrum. Meas. **53**, 1197 (2004).

[24] J. Obrzut, A. Anopchenko, and R. Nozaki, *Proceedings of IEEE Conference on Instrumentation and Measurement*, Ottawa, Canada, 16–19 May 2005, (IEEE, New York, 2005), Vol. 2, p. 1530.

[25] J. C. Dyre and T. B. Shroder, Rev. Mod. Phys. **72**, 873 (2000).

[26] F. Kremer and A. Schonhals, *Broadband Dielectric Spectroscopy*

(Springer, Berlin, 2003), Chap. 2.

[27] J. Obrzut, J. F. Douglas, S. B. Kharchenko, and K. B. Migler, Phys. Rev. B **76**, 195420 (2007).

[28] P. B. Macedo, C. T. Moynihan, and R. Bose, Phys. Chem. Glasses **13**, 171 (1972).

[29] S. A. Chen and C. S. Liao, Macromolecules **26**, 2810 (1993).

[30] A. Meyer, R. D. Dimeo, P. M. Gehring, and D. A. Neumann, Rev. Sci. Instrum. **74**, 2759 (2003).

[31] V. Arrighi, R. Ferguson, R. E. Lechner, M. Telling, and A. Triolo, Physica B **301**, 35 (2001).

[32] V. Arrighi, F. Ganazzoli, C. Zhang, and S. Gagliardi, Phys. Rev. Lett. **90**, 058301 (2003).

[33] N. F. Mott, E. A. Davis, and R. A. Street, Philos. Mag. **32**, 961 (1975).

[34] R. H. M. van de Leur, Synth. Met. **51**, 69 (1992).

[35] R. H. M. van de Leur, B. de Ruiter, and J. Breen, Synth. Met. **57**, 4956 (1993).

[36] K. Yazawa, Y. Inoue, T. Yamamoto, and N. Asakawa, Phys. Rev. B **74**, 094204 (2006).

[37] J. C. Dyre, J. Appl. Phys. **64**, 2456 (1988).

[38] A. K. Joncher, *Universal Relaxation Law* (Chelsea Dielectrics, London, 1996), Chap. 2.7.

[39] W. F. Pasveer, P. A. Bobbert, and M. A. J. Michels, Phys. Rev. B **74**, 165209 (2006).

[40] D. L. Sidebottom, Phys. Rev. Lett. **82**, 3653 (1999).

[41] M. Pollak and T. H. Geballe, Phys. Rev. **122**, 1742 (1961).

[42] M. Ben-Chorin, F. Moller, F. Koch, W. Schirmacher, and M. Eberhard, Phys. Rev. B **51**, 2199 (1995).

[43] O. Bleibaum, E. Haba, H. Bottger, and V. V. Bryksin, Phys. Status Solidi B **241**, 13 (2004).

[44] C. Ganter and W. Schirmacher, Philos. Mag. B **81**, 915 (2001).

[45] S. Havriliak Jr. and S. J. Havriliak, J. Polym. Sci., Part B: Polym. Phys. **35**, 1887 (1997).

[46] *Dielectric Properties of Amorphous Polymers*, edited by J. P. Runt and J. J. Fitzgerald (Am. Chem. Soc., Washington, DC, 1997), Chap. 3.

[47] P. Hedvig, *Dielectric Spectroscopy of Polymers* (John Wiley & Sons, New York, 1997).

[48] B. Frick and L. J. Fetters, Macromolecules **27**, 974 (1994).

[49] A. Sanz, M. Ruppel, J. F. Douglas, and T. Cabral, J. Phys.: Condens. Matter **20**, 104209 (2008).

[50] J. J. M. van der Holst, M. A. Uijttewaal, B. Ramachandhran, R. Coehoorn, P. A. Bobbert, G. A. deWijs, and R. A. deGroot, Phys. Rev. B **79**, 085203 (2009).

[51] A. Troisi, D. L. Cheung, and D. Andrienko, Phys. Rev. Lett. **102**, 116602 (2009).

[52] A. R. Long and N. Balkan, J. Non-Cryst. Solids **35-36**, 415 (1980).

[53] B. Popescu and A. R. Long, Phys. Status Solidi **205**, 141 (1998).

[54] J. R. Macdonald, J. Appl. Phys. **62**, R51 (1987).

[55] H. Bottger and V. V. Bryksin, *Hopping Conduction in Solids* (Akademie-Verlag, Berlin, 1985), Chap. 6.4.

[56] G. Dicker, M. P. de Haas, D. M. de Leeuw, and L. D. A. Siebbeles, Chem. Phys. Lett. **402**, 370 (2005).

[57] L. G. Kaake and X. Y. Zhu, J. Phys. Chem. C **112**, 16174 (2008).